

# **A STUDY OF REACTION DIFFUSION EQUATIONS FOR BIOLOGICAL PATTERN FORMATION**

*A Project Report*

*submitted by*

**JAYADEV BHASKARAN**

*in partial fulfilment of the requirements  
for the award of the degree of*

**BACHELOR OF TECHNOLOGY**



**DEPARTMENT OF ELECTRICAL ENGINEERING  
INDIAN INSTITUTE OF TECHNOLOGY MADRAS.**

**May 2014**

## THESIS CERTIFICATE

This is to certify that the thesis titled **A STUDY OF REACTION DIFFUSION EQUATIONS FOR BIOLOGICAL PATTERN FORMATION**, submitted by **JAYADEV BHASKARAN**, to the Indian Institute of Technology, Madras, for the award of the degree of **Bachelor of Technology**, is a bona fide record of the research work done by him under our supervision. The contents of this thesis, in full or in parts, have not been submitted to any other Institute or University for the award of any degree or diploma.

**Dr. R. Aravind**  
Project Guide  
Professor  
Dept. of Electrical Engineering  
IIT-Madras, 600 036

Place: Chennai

Date: 8<sup>th</sup> May 2014

## **ACKNOWLEDGEMENTS**

At the outset, I would like to sincerely thank Dr. R. Aravind, my project guide and professor at IIT Madras. He was more than just a project guide - an enthusiastic professor, a mentor and a person ready to help me out with any difficulties I faced. His inputs were instrumental towards shaping the course of this project, and I also got to learn more about research through my interactions with him. I also thank S. N. Sreerag, MS research scholar at the Department of Electrical Engineering, for having guided me through the initial sections of the project. It was very helpful to have the guidance of someone who was working on a similar topic, and this made my progress much smoother than expected.

The last four years at IIT Madras have been a constant learning experience. I thank all my professors, both from the Department of Electrical Engineering and from other departments, whose guidance and teaching has equipped me with the necessary tools and skills to complete this project. I also thank all my friends, whose support and encouragement helped me overcome the hurdles that I faced during the course of the project. Finally, I thank my parents and my brother for all the help and support over the course of my time at IIT Madras.

# TABLE OF CONTENTS

<b>ACKNOWLEDGEMENTS</b>	<b>i</b>
<b>1 INTRODUCTION</b>	<b>2</b>
<b>2 REACTION-DIFFUSION PATTERNS IN ZEBRAFISH</b>	<b>4</b>
2.1 Overview . . . . .	4
2.2 Model and simulations . . . . .	4
2.3 Simulation results . . . . .	6
2.3.1 Variation in patterns with respect to parameter values . . . .	7
2.3.2 Stable and unstable patterns - temporal variations . . . . .	12
2.4 Discussion . . . . .	13
<b>3 REACTION-DIFFUSION BASED EPIDEMIC MODELS</b>	<b>14</b>
3.1 Overview . . . . .	14
3.2 Model and simulations . . . . .	14
3.3 Simulation results . . . . .	16
3.3.1 1-D system . . . . .	16
3.3.2 2-D system . . . . .	20
3.4 Discussion . . . . .	24
3.5 Further work . . . . .	24
<b>4 CONCLUSIONS</b>	<b>26</b>
<b>REFERENCES</b>	<b>27</b>

# CHAPTER 1

## INTRODUCTION

The subject of biology has undergone a change in recent times, with the introduction of mathematical techniques to study biological phenomena. Within mathematical biology, partial differential equations have been used to model and analyze the behaviour of a large variety of systems. These include things as diverse as population dynamics, predator-prey models, biological pattern formation and the spread of diseases. Murray (2002), one of the fundamental texts on mathematical biology, lists a variety of fields in which such systems of equations can be seen. This thesis deals with the investigation of two such applications of reaction-diffusion equations, namely zebrafish stripe patterns and epidemic models.

The use of reaction-diffusion equations to model biological coat patterns (such as patterns seen on fish, tigers, zebras and other organisms) was first used during the 1950s. Alan Turing's seminal work in this field (Turing (1952)) was one of the first works to discuss the mathematical basis of the underlying chemical reactions behind pattern formation. Murray (2002) also describes detailed mathematical models for mammalian coat patterns, such as those seen on tigers and zebras. Works such as Kondo and Asai (1995), Asai *et al.* (1999) and Kondo and Miura (2010) have concentrated specifically on reaction-diffusion models for fish patterns. In Chapter 2, a mathematical model for zebrafish stripe patterns (based on Asai *et al.* (1999)) was analyzed, and the effects of varying the parameters was studied. The stability of different types of zebrafish patterns was also investigated. This work can help to understand the relationship between the parameters and the expressed patterns, and can be used by biologists to gain insights into the mathematical models describing morphogenesis.

The use of mathematical models to study epidemics is one of the most application-oriented areas of mathematical biology. With rising populations and increasing congestion in urban localities, it has become very easy for diseases to be transmitted across regions. Mathematical models to study the spread of diseases such as cholera and typhoid have been constructed, such as in Capasso and Paveri-Fontana (1979), which

dealt with cholera in Mediterranean Europe. In Chapter (3), a reaction-diffusion model for man-environment-man epidemics was studied, and the role of each parameter was investigated. The response to an outbreak of the disease was simulated for various conditions. Such models can be used to estimate the possible damage that could be caused by an epidemic, and design measures to prevent it from spreading. Some ideas on further extensions along similar lines were also proposed.

All simulations shown in the thesis were done using (MATLAB (2010)), and this thesis was prepared using  $\text{\LaTeX}$ .

## CHAPTER 2

# REACTION-DIFFUSION PATTERNS IN ZEBRAFISH

### 2.1 Overview

As mentioned earlier, the theory of reaction diffusion equations can be used to model pattern generation on animal bodies. Earlier works such as Kondo and Asai (1995) and Asai *et al.* (1999) have looked at fish stripe patterns using reaction-diffusion systems. Using the model proposed in Asai *et al.* (1999), simulations were performed in order to determine the variations in stripe patterns on the bodies of zebrafish. The wide variety of stripe patterns obtained by varying the parameter values in the models was in keeping with the variety of stripe patterns seen on zebrafish.

The theory, as explained in Asai *et al.* (1999), states that a mutation resulting in the structure of the catalyzing enzymes (for the reaction diffusion system) can be represented by a change in parameters from the original model. Thus, starting from the same initial condition (three horizontal white stripes, in our case), it was possible to obtain various other patterns (stripes, spots, irregular patterns) by varying the parameters.

Furthermore, patterns were found to be of two types - stable and oscillatory. The stable patterns resulted in steady diffusion of the same original stripe pattern, while oscillatory patterns showed some periodic variations between white stripes on a black background and black stripes on a white background. This was possibly due to the relative values of the coefficients used in the system of PDEs.

The model was proposed for zebrafish, with modifications in *Leopard* gene. Similar reaction diffusion models can also be used to describe patterns in various other biological situations.

### 2.2 Model and simulations

The underlying model used was as follows (as described in Asai *et al.* (1999)):

$$\frac{\partial u}{\partial t} = x(u, v) - du + D_u \nabla^2 u$$

$$\frac{\partial v}{\partial t} = y(u, v) - gv + D_v \nabla^2 v$$

$$x(u, v) = au - bv + c$$

$$y(u, v) = eu - f$$

$$0 \leq x, y \leq P$$

In this model,  $u$  and  $v$  represent the concentrations of two chemical species known as the activator and the inhibitor. The parameters  $a, b, c, d, e, f$  and  $g$  were varied in order to generate different zebrafish patterns.  $D_u$  and  $D_v$  represent the diffusion coefficients for the activator and the inhibitor respectively.  $P$  represents the maximum threshold on the value of both activator and inhibitor concentrations.

The  $\nabla^2$  operation was implemented using the five-point stencil finite difference method, a commonly used implementation of the discrete Laplacian operator with step size  $h$ .  $\nabla^2 u(x, y) = (u(x-h, y) + u(x+h, y) + u(x, y-h) + u(x, y+h) - 4 \times u)/h^2$

Since the exact values of most of these parameters cannot be determined analytically, the results of the simulations must be treated as qualitative, rather than quantitative. The trends observed were due to relative, rather than absolute, values of the parameters.

To begin with, the initial pattern was specified as 3 white stripes across the body (as shown in Figure 2.1), by setting a high value of the activator in those regions of the grid. The simulations (in each case) were run for 10000 cycles, on a  $100 \times 100$  grid with a granularity of 0.1. A high activator concentration was depicted by 'white' regions, and a low concentration by 'black' regions on the plots.

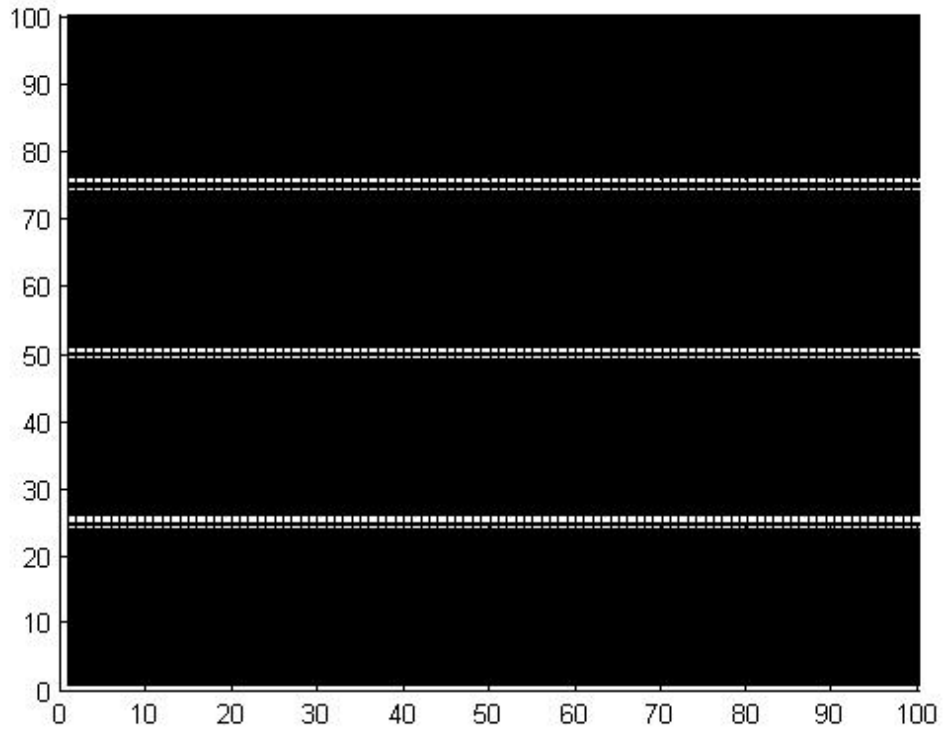


Figure 2.1: Initial Stripe Pattern

## 2.3 Simulation results

To begin with, the following default values were set for the various parameters (as specified in Asai *et al.* (1999)):

$$a = 0.08$$

$$b = 0.08$$

$$c = 0.04$$

$$d = 0.03$$

$$e = 0.10$$

$$f = 0.15$$

$$g = 0.05$$

$$P = 0.50$$

$$D_u = 0.001$$

$$D_v = 0.001$$

All figures show the variation of  $u$  (activator concentration) over the entire range of  $x$  and  $y$  values, after 10000 cycles.

The initial values of the diffusion constants for activator and inhibitor were both set to 0.001. On running the default simulation, the following result was obtained.

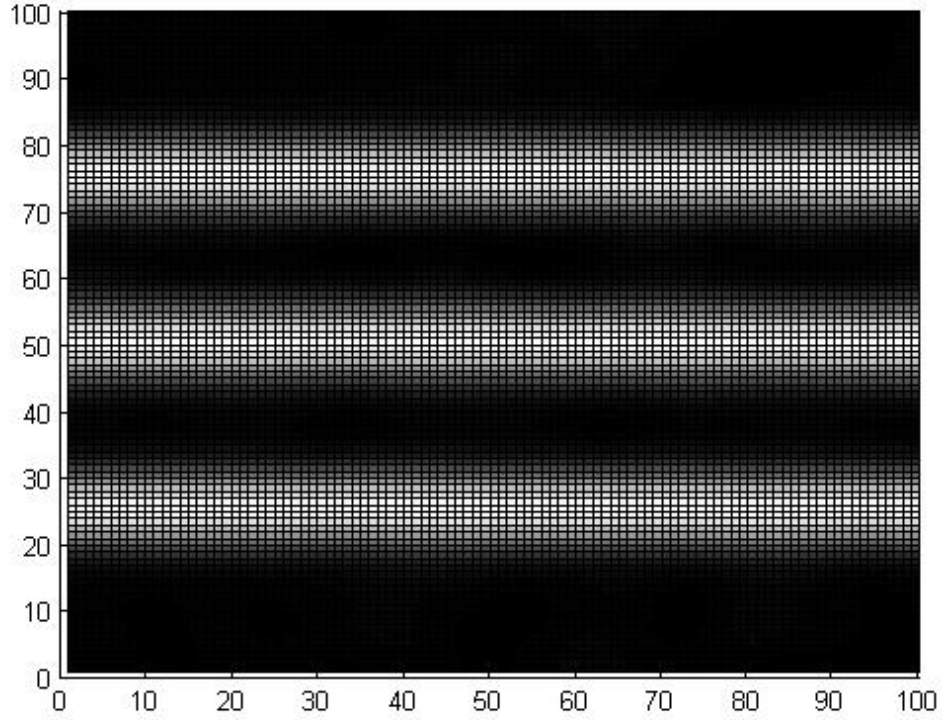


Figure 2.2: Default simulation

As shown in Figure 2.2, the stripes were found to diffuse along the body and become thicker. No significant change was observed beyond this. However, the following simulations (with changing parameter values) showed the range of varied patterns that could be obtained.

### 2.3.1 Variation in patterns with respect to parameter values

The pattern shown in Figure 2.3 was obtained when the value of  $a$  was set to 0.1, keeping all other parameters same. Under these conditions, it was observed that the initial 'white stripe' pattern had transformed into a predominantly grey pattern, with black stripes running along the body of the fish. This resembles the stripe patterns seen in some wild types of zebrafish (experimental data seen in Asai *et al.* (1999))

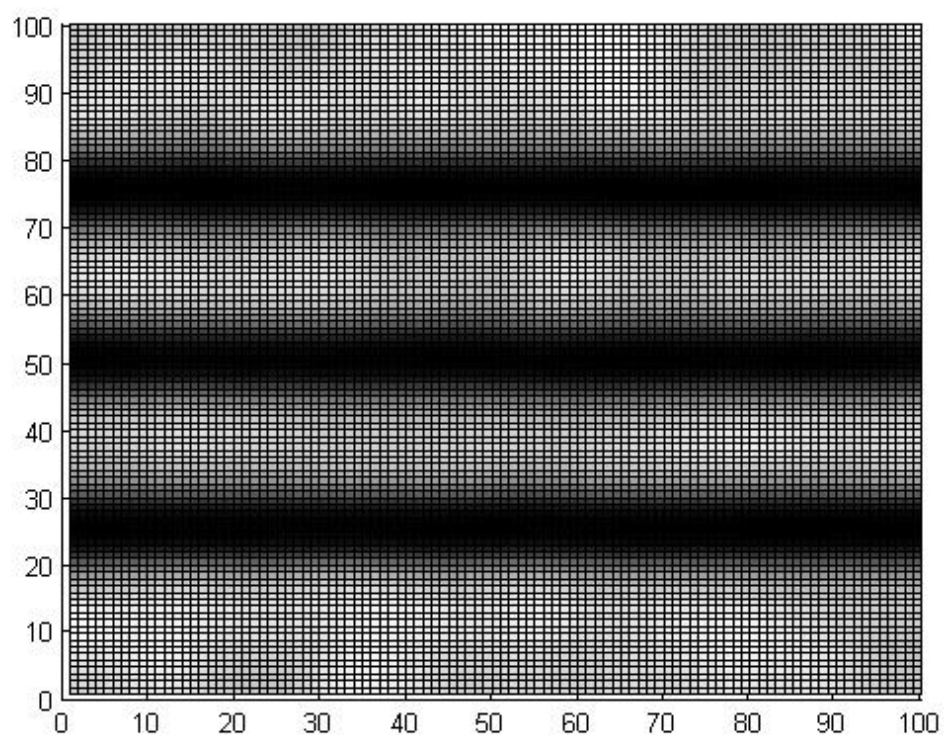


Figure 2.3:  $a = 0.1$

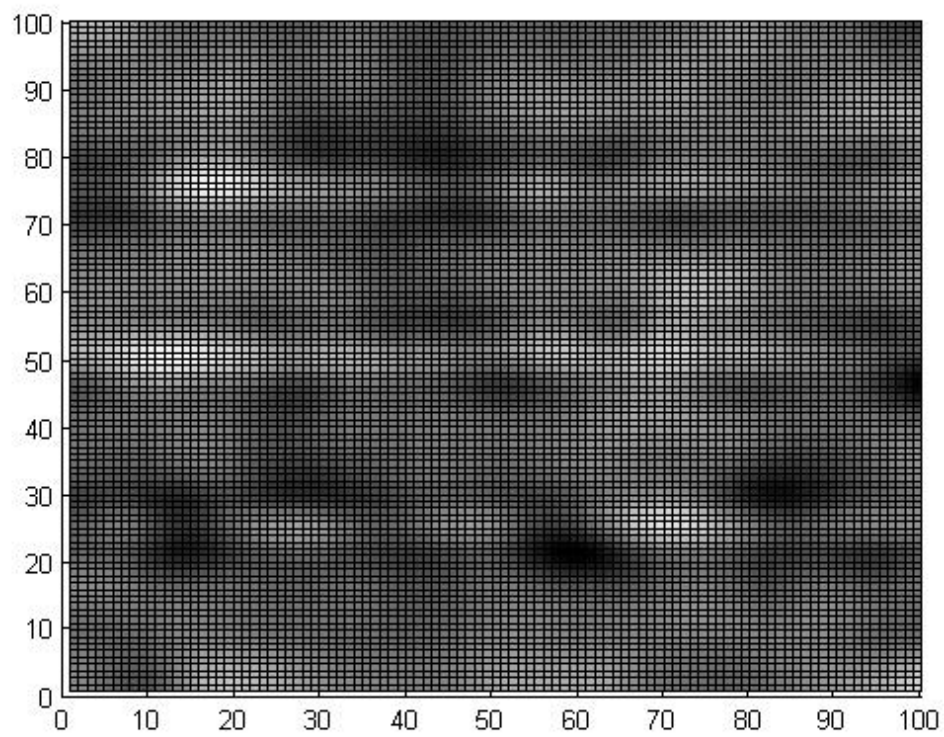


Figure 2.4:  $b = 0.045$

When the parameter  $b$  was reduced to 0.045, the stripes were found to turn extremely faint, with a mottled grey background (as seen in Figure 2.4). Interestingly, the variation in the value of the  $b$  parameter caused no major qualitative change in the stripe pattern till a value of 0.05, following which different patterns were seen. Below a certain threshold (e.g., for  $b = 0.02$ ), the pattern obtained was observed to be identical to the original pattern seen in Figure 2.2.

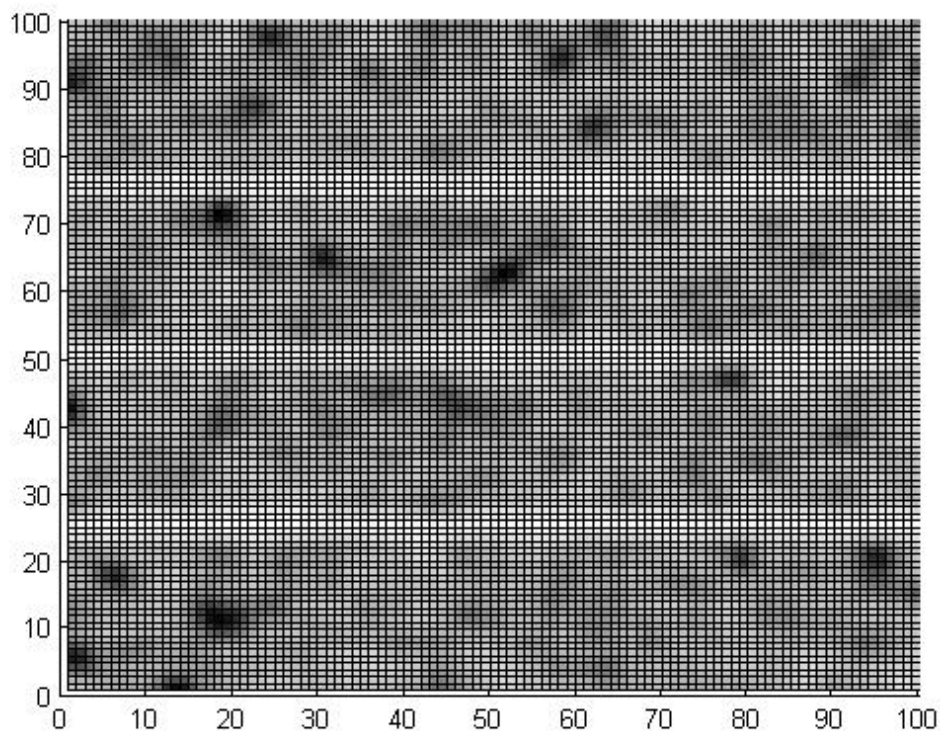


Figure 2.5:  $c = 0.2$

Increasing the value of the parameter  $c$  to 0.2 resulted in a pattern (Figure 2.5) that had black spots on a white background, as seen in certain variants of zebrafish.

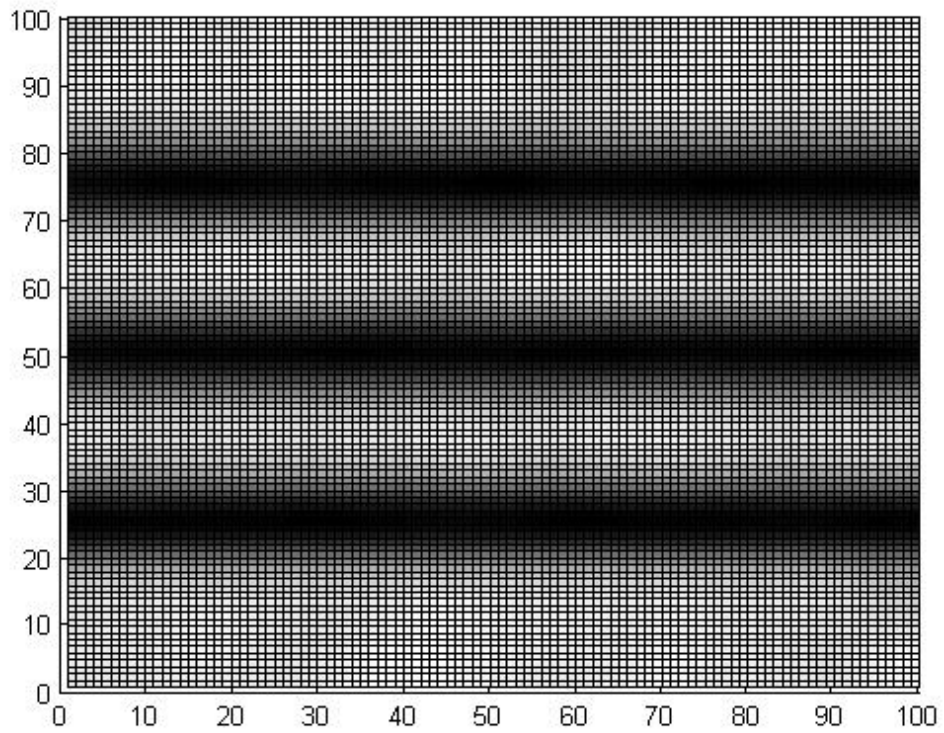


Figure 2.6:  $d = 0.01$

Varying the value of the parameter  $d$  to 0.01 caused the appearance of a pattern (Figure 2.6) showing black stripes on a white background. The stripes, however, were found to be thinner than the ones seen in Figure 2.3, though similar in pattern.

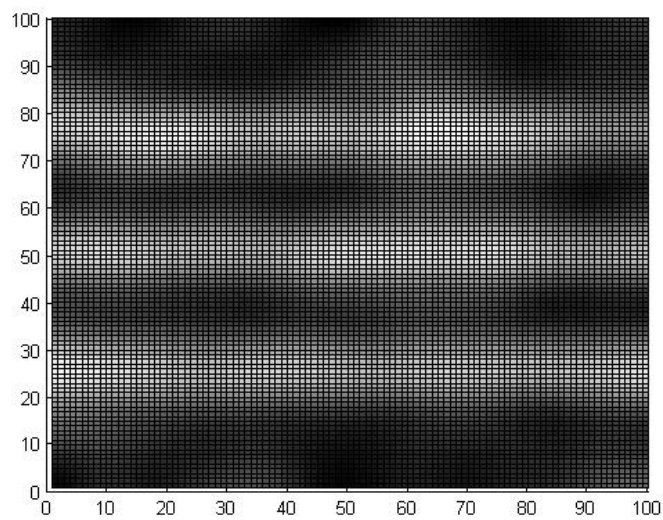


Figure 2.7:  $e = 0.08$

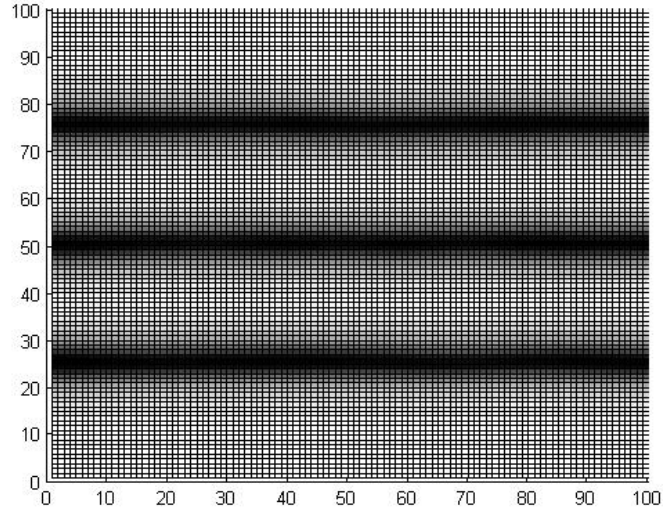


Figure 2.8:  $f = 0.2$

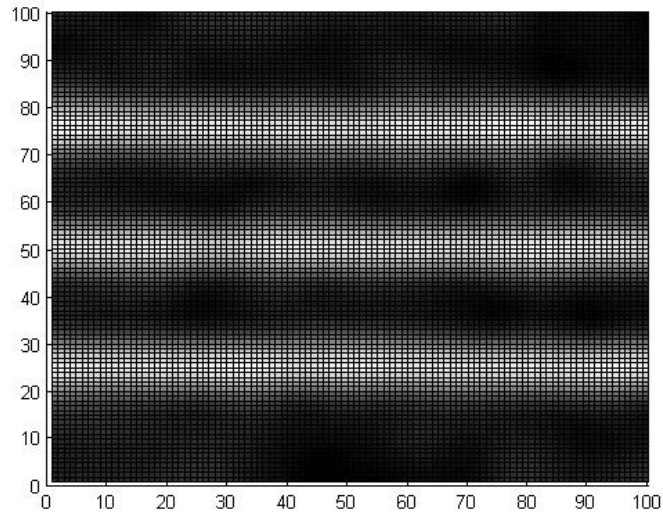


Figure 2.9:  $g = 0.08$

When the parameter  $e$  was reduced to 0.08, the stripes became wider as well as fainter when compared to the original pattern. Some of the stripes became less distinct and merged to form a larger white pattern, interspersed with black regions (Figure 2.7).

When  $f$  was increased to 0.2, the pattern formed (Figure 2.8) again showed black stripes on a white background (similar to Figure 2.6 and Figure 2.6). These stripes were found to be thinner than the ones in Figure 2.6 and much thinner than the ones in Figure 2.3.

Increasing  $g$  to 0.08 (as shown in Figure 2.9) resulted in a slightly distorted version of the stripe pattern with the original set of parameters (shown in Figure 2.2).

### 2.3.2 Stable and unstable patterns - temporal variations

Another interesting feature that was observed was the stability of certain patterns. While some sets of parameters gave rise to patterns that were stable and kept evolving in the same manner with respect to time, others gave rise to unstable patterns that varied from one set of features to another with a certain periodicity. Stability in patterns was observed whenever the value of  $u$  saturated (due to  $x(u)$  reaching either 0 or  $P$ ). This periodic variation in patterns is also seen in other biological systems, such as predator-prey species described by the Lotka-Volterra logistic equations.

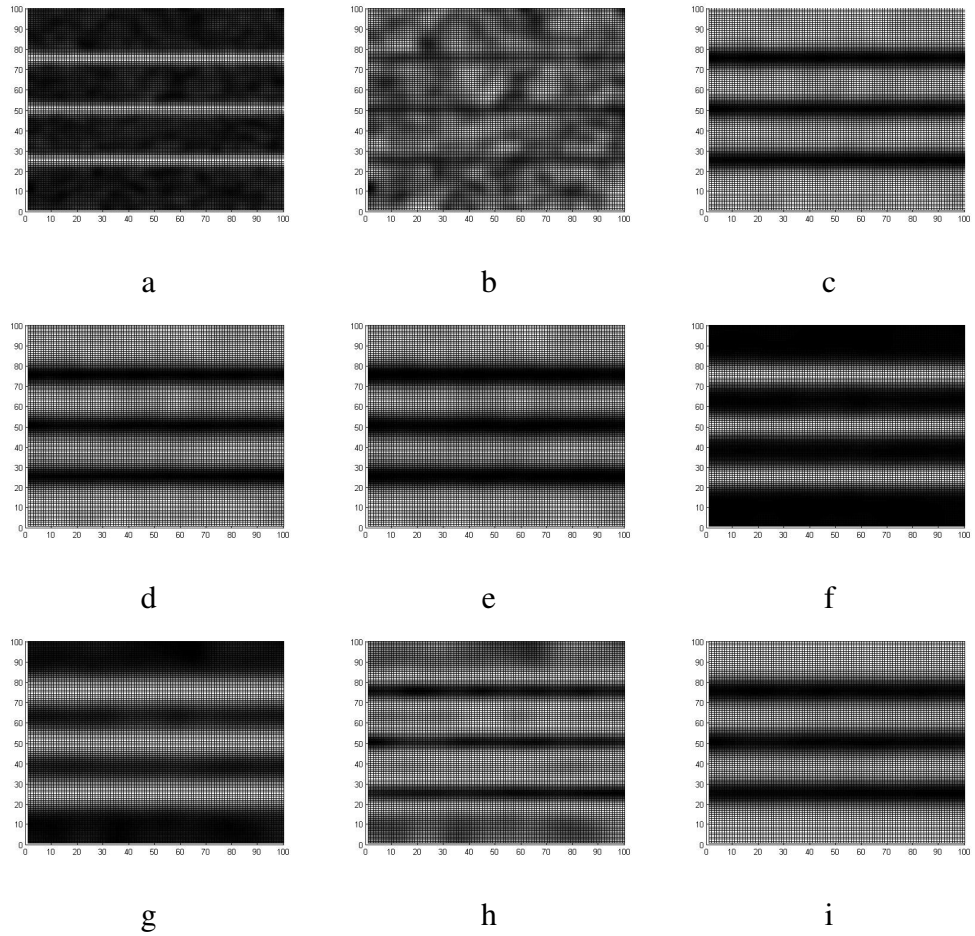


Figure 2.10: oscillatory patterns (a-i)

Simulation results showed both types of patterns (stable patterns and oscillating patterns), as shown in Figure 2.10 and Figure 2.11 respectively.

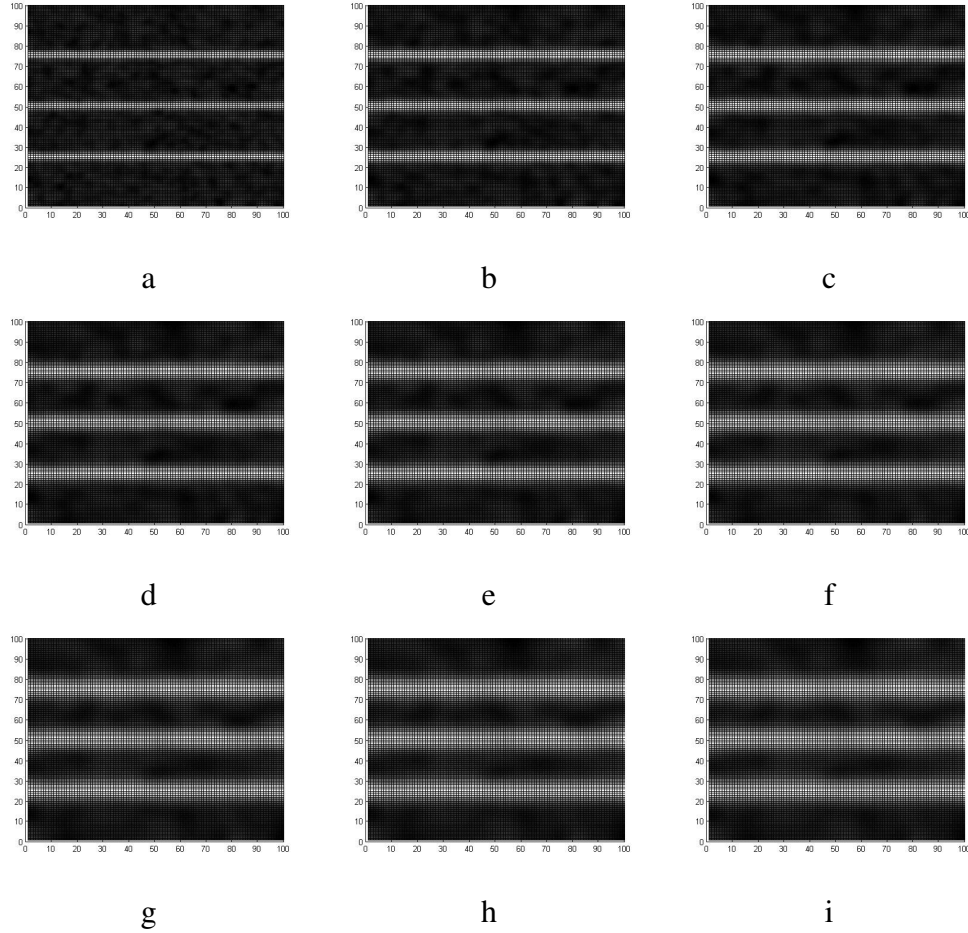


Figure 2.11: Stable patterns (a-i)

## 2.4 Discussion

First, the variations in zebrafish stripe patterns with respect to the parameters in the model were studied, and different patterns (observable in zebrafish) were generated by varying the parameters. This could be extended by looking at thresholding effects. Many organisms apply some sort of biological thresholding in order to come up with black and white patterns (e.g., zebras), and this could be done in our case also. Furthermore, the exact relationship of the various parameters to the expression of the underlying genes could be investigated (similar to what has been done in Asai *et al.* (1999)).

Then, the stability of the patterns with respect to time was studied. Further work could involve looking at the exact time scales and parameter values that determine stability of patterns, and the biological rationale behind the stability, or lack thereof, of particular sets of patterns. Also, the model here was defined for zebrafish - one could try to investigate similar models for other organisms and attempt to come up with some general results that could give further insight into the theory of animal patterns.

## **CHAPTER 3**

# **REACTION-DIFFUSION BASED EPIDEMIC MODELS**

### **3.1 Overview**

The mathematical treatment of epidemic spreading is another area where reaction diffusion equations can be applied. The spread of infectious diseases depends on the distribution of the infectious agents as well as the distribution of the affected human population. Certain models of epidemic spreading have also incorporated the geographical spread of the agents (vectors) using reaction-diffusion models. The model used as the basis for the simulations in this section was from Capasso and Kunisch (1988). Phenomena relating to the spread of numerous transmittable diseases, such as cholera, typhoid fever and malaria have been studied using similar models.

In this section, the reaction-diffusion model for the man-environment-man epidemic model was studied, and the effect of varying the model parameters was investigated. The theory, as stated in Capasso and Kunisch (1988) and Capasso and Wilson (1997), concerns the variation in concentration of infectious agents as well as the percentage of affected humans, and also deals with the spatial spreading of the infectious agents. Simulations were performed, starting with an initial localized epidemic outbreak, and the subsequent behaviour was studied for a range of parameters. These simulations were performed for a one-dimensional system and later extended to the two-dimensional systems, and the results were obtained. In certain cases, the epidemic was localized to the initial affected region and gradually died out, while in other cases the epidemic spread across the entire simulation space.

### **3.2 Model and simulations**

The following model was used as the underlying basis for the simulations:

The underlying model used was as follows (as described in Capasso and Kunisch (1988)):

$$\frac{\partial u}{\partial t} = D\nabla^2 u(x, t) - a_{11}u(x, t) + a_{12}v(x, t)$$

$$\frac{\partial v}{\partial t} = a_{21}g(u(x, t)) - a_{22}v(x, t)$$

Here,  $u$  represents the concentration of the infectious agent species in the environment, while  $v$  represents the infective human population at a particular spatial location, at a particular point in time. The parameters  $a_{11}$  and  $a_{22}$  represent the reciprocal of the mean lifetime of the infectious agent and the reciprocal of the mean infectious period (on humans) respectively. The parameter  $a_{12}$  is the multiplicative factor of the infectious agent due to the human population at a particular location, while the function  $g(u)$  represents the 'force of infection', as described in Capasso and Wilson (1997).  $D$  represents the diffusion constant for the infectious agent species.

The function  $g$  can be chosen as any monotonically increasing function such that  $g(0) = g'(0) = 0$ ,  $g'(x)$  is positive for any  $x > 0$ ,  $\lim_{x \rightarrow \infty} g(x) = 1$  and  $g$  has a transition from convex to concave at some point  $x_0 > 0$ . In all the simulations, the choice of  $g$  was taken as  $g(x) = x^2/(1 + x^2)$ .

In the 1-D case ( $x = 0$  to  $x = 100$ ), the initial condition was set at random and scaled to a lower value ( $u = 0.05 \times rand(100)$ ) throughout the line, with the corresponding value of  $g$  as the initial condition for  $v$  ( $v = g(u)$ ). The epidemic outbreak was then simulated with a pulse of value  $u_0$  at  $x = 50$  and  $x = 51$ . The values of the parameters were varied and the resulting situation was represented in the form of graphs, showing the evolution of  $u$  as a function of space and time.

In two dimensions,  $u(x, t)$  and  $v(x, t)$  were replaced by  $u(x, y, t)$  and  $v(x, y, t)$ . The system was simulated on a grid of size  $100 \times 100$ . The initial conditions were taken as  $u = 0.05 \times rand(100, 100)$  and  $v = g(u)$ . The epidemic outbreak was then simulated with a pulse of value  $u_0$  localized from  $(x, y) = (50, 50)$  and  $(x, y) = (51, 51)$ . A similar investigation of parameter variation effects was performed, and the resulting surface graphs were plotted.

### 3.3 Simulation results

#### 3.3.1 1-D system

The first set of results below show the variation in the concentration of the infecting species ( $u$ ) over the entire simulation space ( $x = 0$  to  $x = 100$ ), at various points of time.

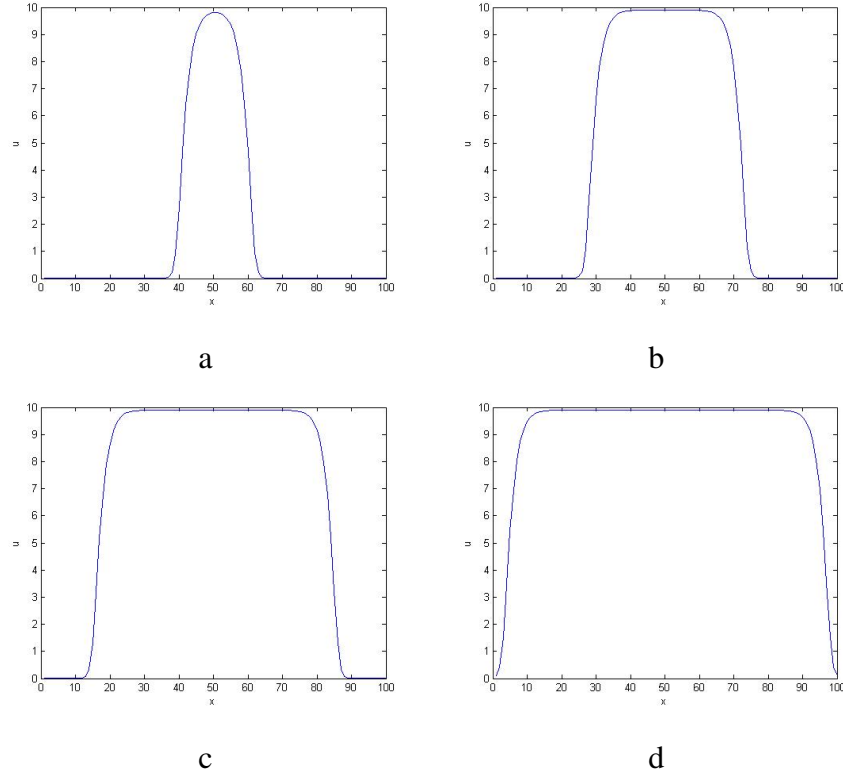


Figure 3.1:  $u(x)$  versus loop iterations: (a)1000 iterations, (b)2000 iterations, (c)3000 iterations, (d)4000 iterations

Initially, the following conditions were specified:  $a_{11} = a_{21} = a_{22} = 0.01$ ,  $a_{12} = 0.1$ ,  $D = 0.01$  and  $u_0 = 1$ . On simulating the system, the concentration of  $u$  as a function of distance was determined (as shown in Figure 3.1). All following plots show the variation of infecting species concentration ( $u$ ) over the entire simulation space ( $x=0$  to  $x=100$ ), after 2000 iterations.

When the value of the parameter  $a_{11}$  was varied, the behaviour of the system showed the following trend: the final value of  $u$  varied inversely with the value of  $a_{11}$ , as shown in Figure 3.2.

When  $a_{12}$  was varied, the following trends were observed. A higher parameter value

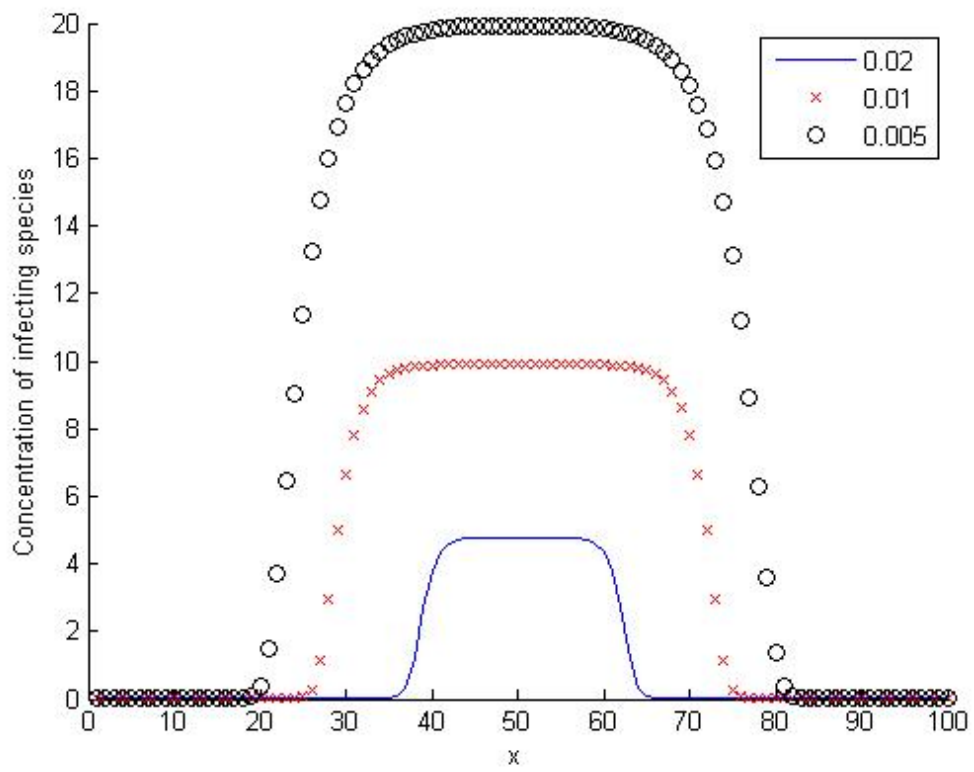


Figure 3.2: Variation of  $u$  for different values of  $a_{11}$

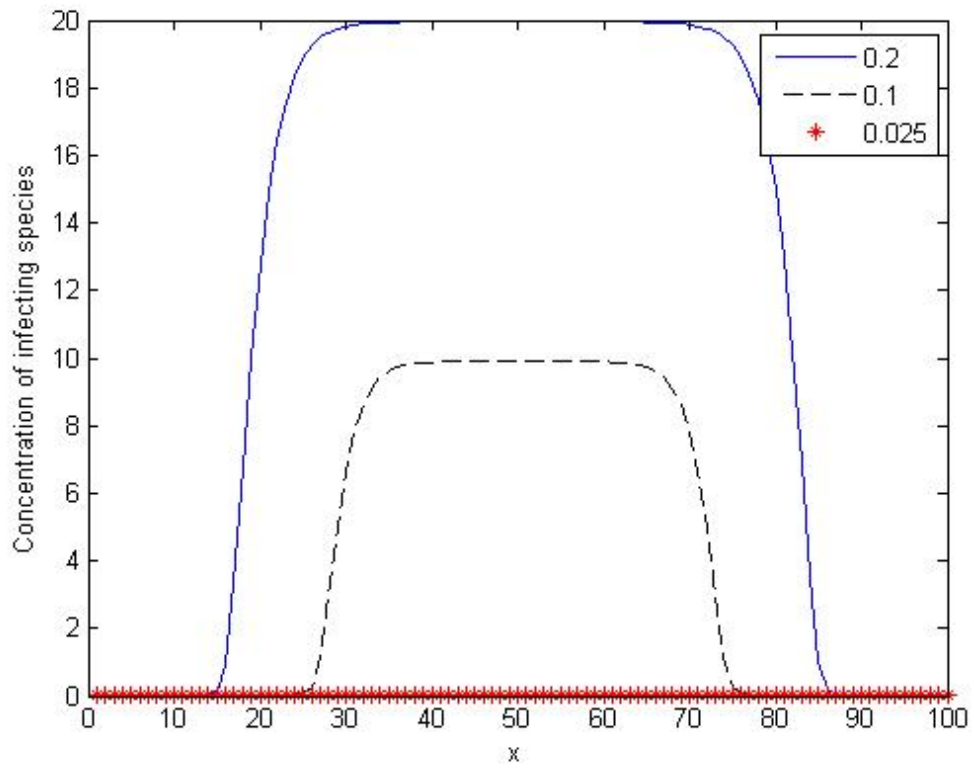


Figure 3.3: Variation of  $u$  for different values of  $a_{12}$

resulted in a higher saturation level, as well as more infected regions for the same initial condition. Also, below a certain value, the disease dies out and does not spread at all (e.g.,  $a_{12} = 0.025$ , as shown in Figure 3.3).

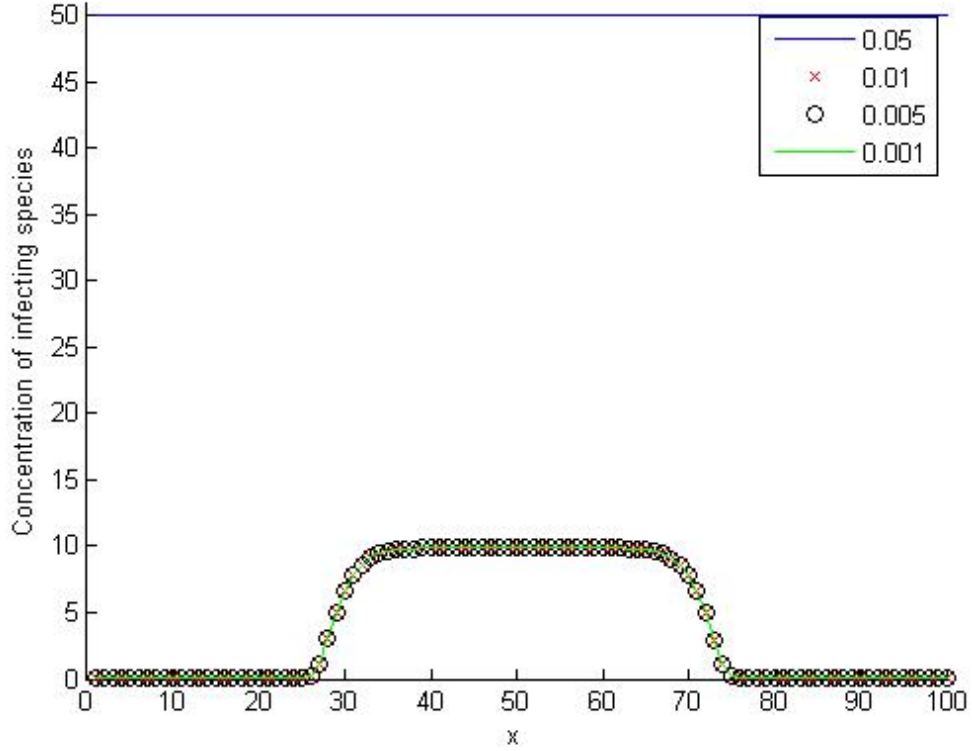


Figure 3.4: Variation of  $u$  for different values of  $a_{21}$

The variation of  $a_{21}$  showed some interesting properties (Figure 3.4). Above a certain threshold, any increase in the value of the parameter led to a corresponding increase in the final saturation value, as well as the area infected. However, reducing the value of the parameter had no effect below a certain point (with other parameters staying constant). In our case, parameter values of 0.01, 0.005 and 0.001 all showed the same behaviour.

When  $a_{22}$  was varied, the following behaviour was observed (Figure 3.5). On reducing the value of the parameter, the concentration of the infecting species was found to increase. Increasing the value of the parameter beyond a certain point ensured that the disease died out without spreading. This behaviour was similar to that observed in Figure 3.3.

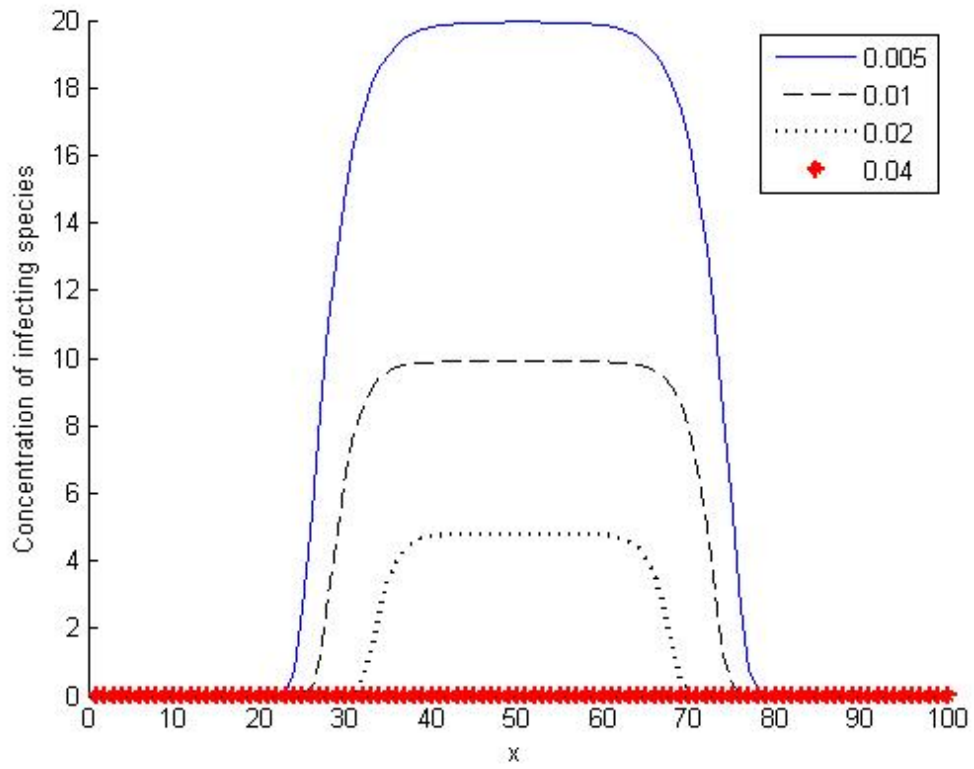


Figure 3.5: Variation of  $u$  for different values of  $a_{22}$

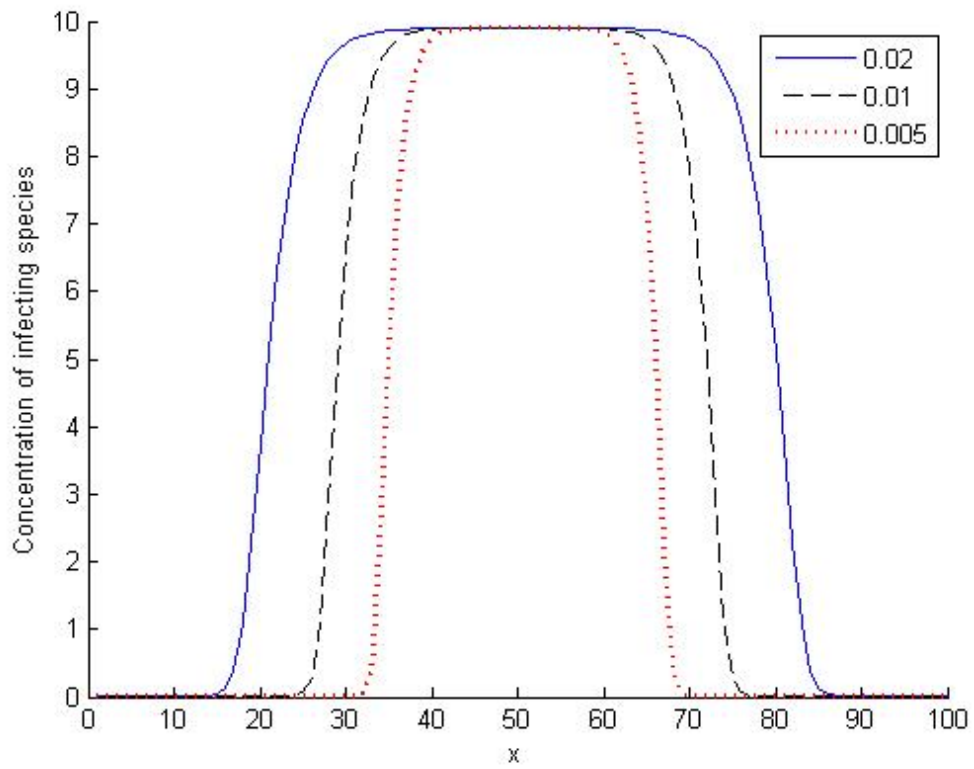


Figure 3.6: Variation of  $u$  for different values of  $D$

Varying the value of the diffusion constant, as expected, resulted in a corresponding

change in the infected area. However, there was no change in the peak concentration of the infecting species (Figure 3.6).

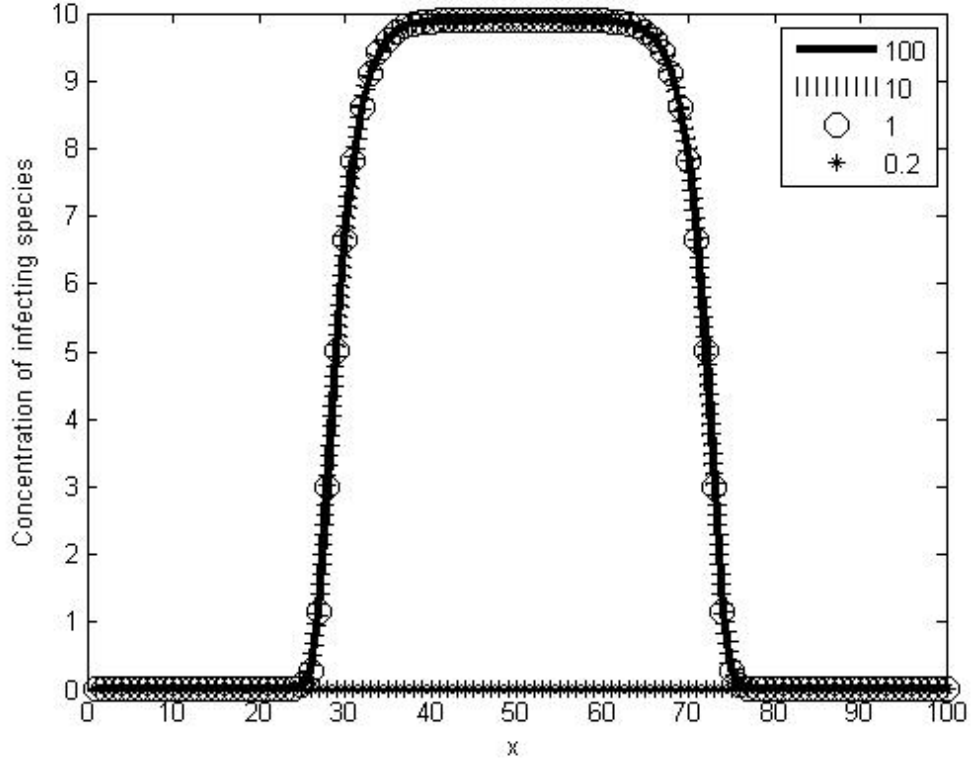


Figure 3.7: Variation of  $u$  for different values of  $u_0$

On the other hand, varying the initial infection pulse ( $u_0$ ) showed an on-off behaviour (Figure 3.7). All values greater than a certain threshold ( $u_0 = 0.33$ ) resulted in the same final state (after a sufficient number of iterations, in this case 2000), while values lower than that threshold ensured that the disease died out. Thus, a bifurcation was seen in the behaviour of the system at a value of  $u_0 = 0.33$ .

### 3.3.2 2-D system

Using the same model as the 1-D system, simulations were performed for a two-dimensional case (as an extension of the same 1-D model). The same initial conditions were specified:  $a_{11} = a_{21} = a_{22} = 0.01$ ,  $a_{12} = 0.1$ ,  $D = 0.01$  and  $u_0 = 1$ . The first set of results below show the variation in the concentration of the infecting species ( $u$ ) over the entire simulation space, at various points of time.

The variation in  $u$  with respect to time was plotted, as shown in Figure 3.8.

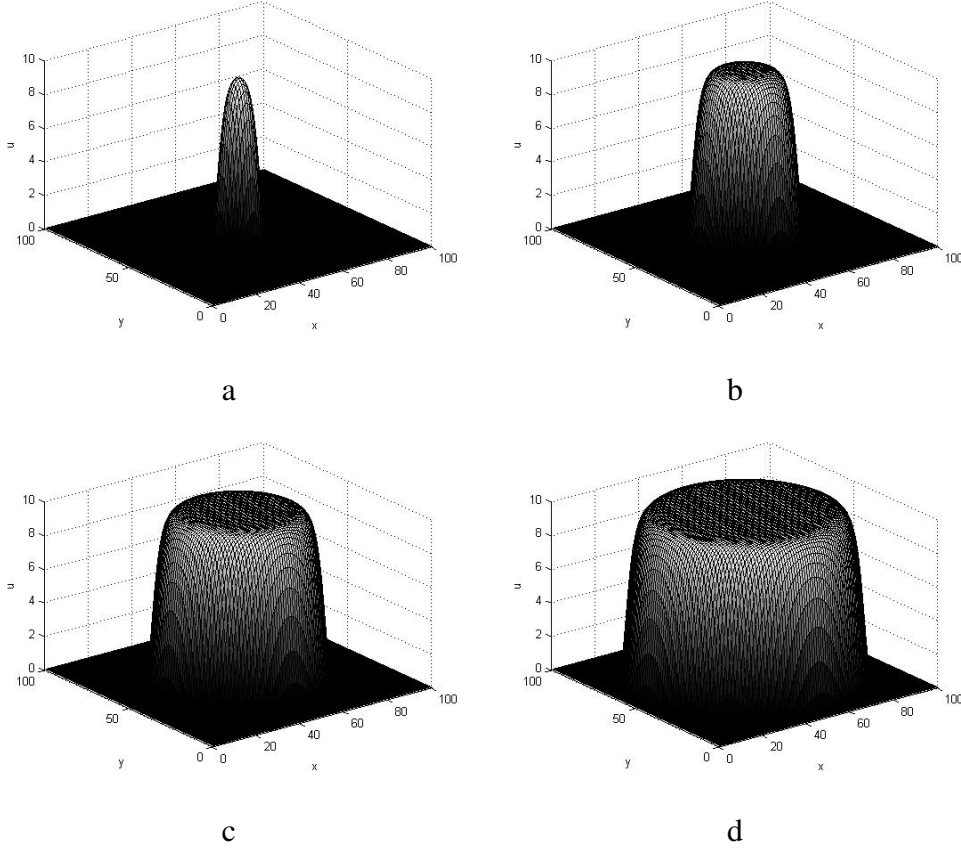


Figure 3.8:  $u(x, y)$  versus loop iterations: (a)1000 iterations, (b)2000 iterations, (c)3000 iterations, (d)4000 iterations

All following plots show the variation of infecting species concentration ( $u$ ) over the entire simulation space ( $x=0$  to  $x=100$ ), after 2000 iterations.

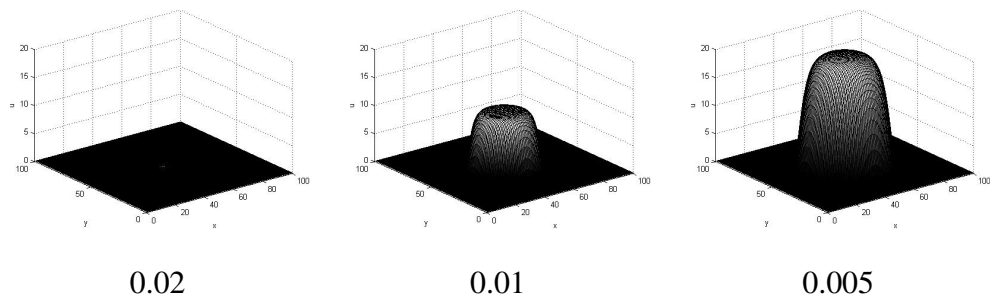


Figure 3.9:  $u(x, y)$  for different values of  $a_{11}$

When the parameter  $a_{11}$  was varied, the following behaviour was observed. Above a certain level, increasing the value of the parameter resulted in zero epidemic spread. Below that threshold value, any reduction in the parameter resulted in an increase in the peak concentration of the infecting species (Figure 3.9).

Varying the value of  $a_{12}$  (Figure 3.10) showed the opposite trend as seen with  $a_{11}$ .

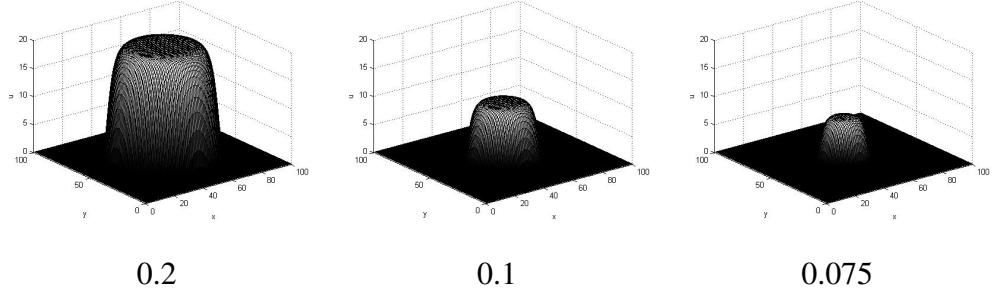


Figure 3.10:  $u(x, y)$  for different values of  $a_{12}$

The value of the parameter was found to be directly proportional to the peak concentration of infecting species. Also, reducing the value below a certain limit resulted in the epidemic dying out. Additionally, an increase in the parameter value also resulted in an increase in the area affected.

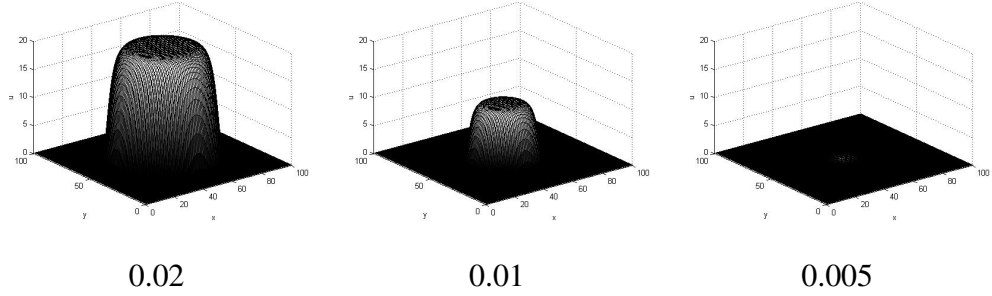


Figure 3.11:  $u(x, y)$  for different values of  $a_{21}$

When  $a_{21}$  was varied, the peak concentration of the infectious agent became higher with a higher parameter value. Also, parameter values below a certain level ensured that the disease died out without spreading (Figure 3.11).

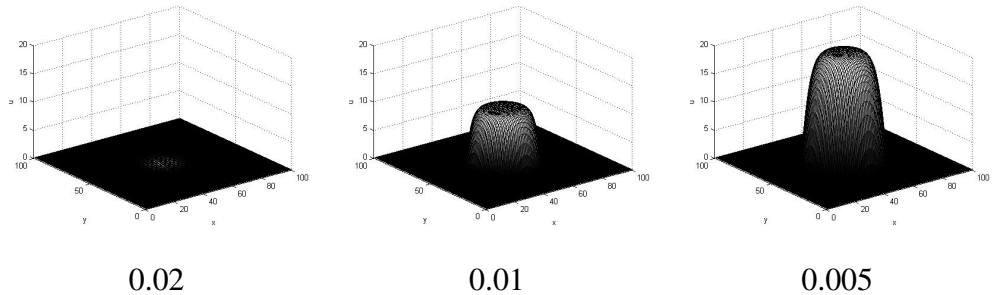


Figure 3.12:  $u(x, y)$  for different values of  $a_{22}$

Varying  $a_{22}$  showed the exact opposite behaviour as  $a_{21}$ . The peak concentration stayed zero for values above a particular threshold (e.g, 0.02), while it increased with a reduction in the parameter value below the threshold (e.g, 0.01, 0.005). This was

plotted, as shown in Figure 3.12. However, there was little correlation between the parameter value and the area affected by the disease.

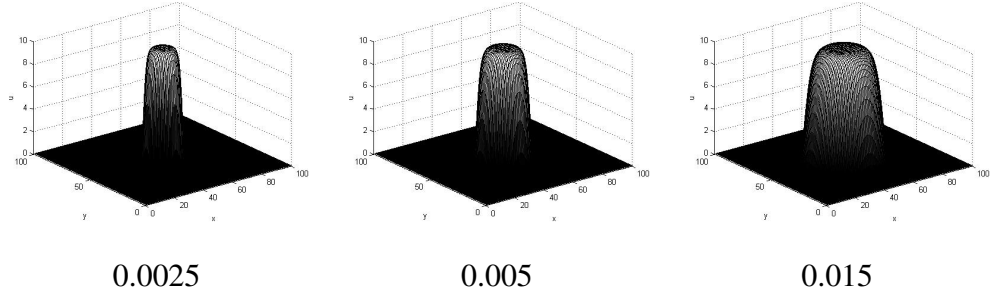


Figure 3.13:  $u(x, y)$  for different values of  $D$

As in the 1-D case, the variation in the diffusion constant  $D$  did not cause any change in the peak concentration of the infecting species. The only change was in the area affected by the disease (Figure 3.13).

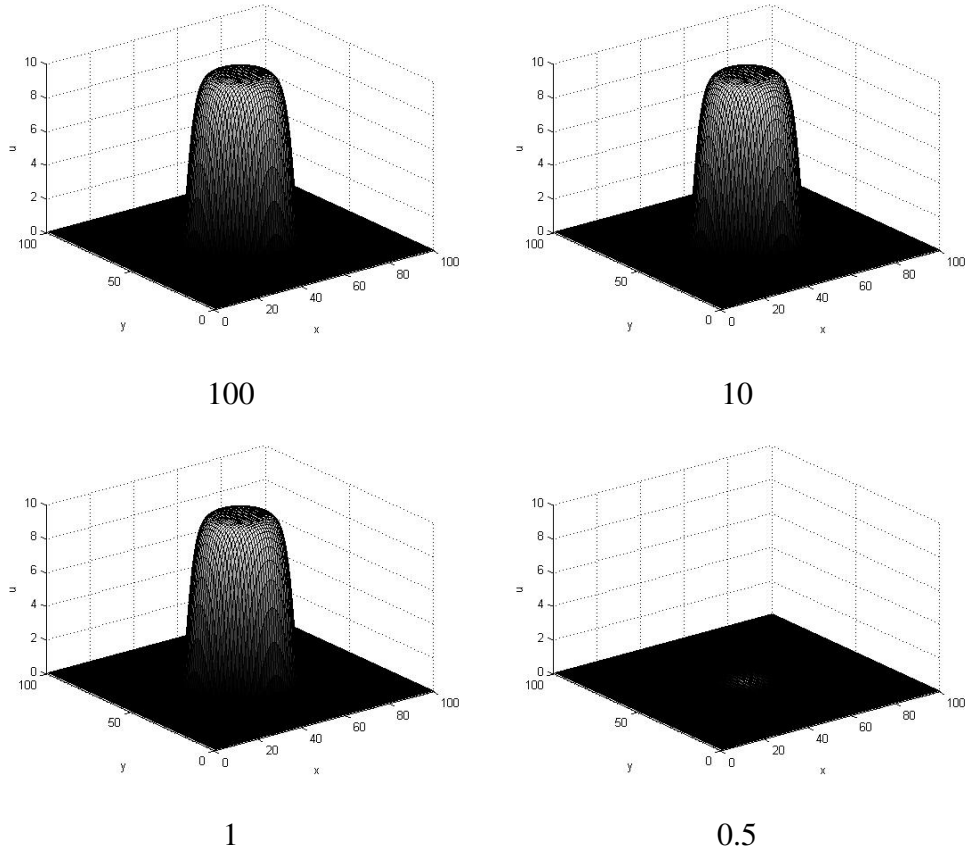


Figure 3.14:  $u(x, y)$  for different values of initial pulse  $u_0$

The variation of  $u$  with respect to the initial infection pulse  $u_0$  also showed a similar behaviour to that of the 1-D analogue. Above a certain threshold value (around 0.6), the system finally stabilized at the same peak value irrespective of the value of  $u_0$ . However,

if the initial pulse was below this threshold, the disease failed to spread and died out (as shown in Figure 3.14).

### 3.4 Discussion

The following trends were seen in general, with respect to both the 1-D and 2-D systems. A higher mean lifetime (lower  $a_{11}$ ) meant that, on an average, the concentration of the agent would be higher. Similarly, a higher infectious period (lower  $a_{22}$ ) was seen to have had the same effects on the system. When the multiplicative factor of the agent was made higher (higher  $a_{12}$ ), the concentration was also found to increase. Furthermore, increasing  $a_{21}$ , which led to an increased effect of the 'force of infection' ( $g$ ) also increased the concentration of the infecting species.

Apart from these factors, the diffusion coefficient  $D$  just controlled the rate of disease spreading, and not the value of the infecting species concentration. The initial disease pulse  $u_0$  served as a switch: any value above a certain threshold was sufficient to trigger an outbreak that could spread to other regions, while any value below the threshold ensured that the disease did not spread.

### 3.5 Further work

Since these models are applicable to many common infectious diseases, they can be used to predict the effects of disease outbreak on populations, similar to Capasso and Paveri-Fontana (1979), which used a similar model to analyze the outbreak of cholera in Mediterranean Europe. Using values for these parameters (determined from previous epidemiological data), these models can be used to assess the amount of damage that could be caused by a particular disease in a particular geographical area. Furthermore, responses can be designed based on which areas are likely to get affected more.

Models that take the effect of medical relief can also be formulated, in order to study how and where medical aid could best be introduced (in the event of an outbreak). One could also simulate several diseases and determine the limits of parameter tolerances for them. Using these limits, we can seek to redesign our existing infrastructure to restrict

the effects of an epidemic to the minimum possible, and prevent them from spreading throughout the area.

## CHAPTER 4

### CONCLUSIONS

In Chapter 2, the reaction-diffusion system governing zebrafish stripe patterns was investigated. The values of the various parameters were tweaked in order to come up with different types of patterns, similar to the ones seen in zebrafish with a modified *Leopard* gene. The qualitative trends seen in the results of these simulations were in keeping with similar results from earlier works such as Asai *et al.* (1999). Furthermore, two broad classes of patterns were determined - stable patterns and oscillatory patterns. Simulations were performed to show examples for each class of patterns. Possible extensions of this part of the thesis include the following - correlating the exact parameter values with the expression of certain genes, comparing the patterns with laboratory organisms and investigating the conditions for stable/oscillatory patterns, and looking at the effect of thresholding on these patterns.

In Chapter 3, the man-environment-man model (described in Capasso and Wilson (1997)) for epidemics was studied, for both one-dimensional and two-dimensional systems. The relationship between the nature of epidemic spreading and the various parameters (mean lifetime of the infectious agent, mean infectious period, multiplicative factor, 'force of infection', diffusion constant and initial infection pulse value) was determined using simulations, for both types of systems. This work can be used to predict the effects of possible future epidemics, and to design appropriate targeted response measures in order to mitigate the damage caused. These models could also be extended to take other factors (such as the effect of medical aid) into account. Simulations could also help to redesign existing areas in order to make it significantly harder for epidemics to spread. This has significant potential, especially in densely populated areas where epidemics can spread quickly and cause a lot of damage.

Thus, mathematical models using reaction-diffusion systems can be used for investigating a variety of biological phenomena. Two such applications have been studied in this thesis, and these were the results of the study.

## REFERENCES

1. **Asai, R., E. Taguchi, Y. Kume, M. Saito, and S. Kondo** (1999). Zebrafish *Leopard* gene as a component of the putative reaction-diffusion system. *Mechanisms of Development*, **89**, 87–92.
2. **Capasso, V. and K. Kunisch** (1988). A reaction-diffusion system arising in modelling man-environment diseases. *Quarterly of Applied Mathematics*, **46**, 431–450.
3. **Capasso, V. and S. L. Paveri-Fontana** (1979). A mathematical model for the 1973 cholera epidemic in the European Mediterranean region. *Revue d'Epidemiologie et de Sante Publique*, **27**, 121–132.
4. **Capasso, V. and R. E. Wilson** (1997). Analysis of a reaction-diffusion system modeling man-environment-man epidemics. *SIAM Journal on Applied Mathematics*, **57**, 327–346.
5. **Kondo, S. and R. Asai** (1995). A reaction-diffusion wave on the skin of the angelfish *Pomacanthus*. *Letters to Nature*, **376**, 765–768.
6. **Kondo, S. and T. Miura** (2010). Reaction-diffusion model as a framework for understanding biological pattern formation. *Science*, **329**, 1616–1620.
7. **MATLAB** (2010). Version 7.10 (R2010a). The MathWorks Inc.
8. **Murray, J. D.**, *Mathematical Biology I: An Introduction*. Springer, 2002.
9. **Turing, A. M.** (1952). The chemical basis of morphogenesis. *Philosophical Transactions of the Royal Society of London. Series B, Biological Sciences.*, **237**, 37–72.